Journal of Power Sources 255 (2014) 266–273

Contents lists available at ScienceDirect

Journal of Power Sources

journal homepage: www.elsevier.com/locate/jpowsour

Leakage current and commutation losses reduction in electric drives for Hybrid Electric Vehicle

El Hadj Miliani*

IFP Energies Nouvelles, 1 et 4 Avenue de Bois Préau, 92500 Rueil-Malmaison, France

HIGHLIGHTS

- Decreasing the global inverter losses by using discontinuous SVPWM techniques.
- Using a new PWM technique which adapt itself to the load characteristics to reduce commutation losses.
- Leakage current sources identification and method to reduce this current.

ARTICLE INFO

Article history:
Received 12 July 2013
Received in revised form
8 November 2013
Accepted 3 January 2014
Available online 15 January 2014

Keywords:
Common-mode
Discontinuous PWM
Leakage current
Switching losses

ABSTRACT

Nowadays, leakage current and inverter losses, produced by adjustable-speed AC drive systems become one of the main interested subject for researchers on Electric Vehicle (EV) and Hybrid Electric Vehicle (HEV) technology. The continuous advancements in solid state device engineering have considerably minimized the switching transients for power switches but the high dv/dt and high switching frequency have caused many adverse effects such as shaft voltage, bearing current, leakage current and electromagnetic interference (EMI). The major objective of this paper is to investigate and suppress of the adverse effects of a PWM inverter feeding AC motor in EV and HEV. A technique to simultaneously reduce the leakage current and the switching losses is presented in this paper. Based on a discontinuous space vector pulse width modulation (DSVPWM) and a modular switches gate resistance, inverter losses and leakage current are reduced. Algorithms are presented and implemented on a DSP controller and experimental results are presented.

1. Introduction

For Electric Vehicle (EV) and Hybrid Electric Vehicle (HEV) drive-train, the inverter controls the electric motor, this is a key component in the vehicle as it determines driving behaviour. The inverter is often controlled by Pulse Width Modulation (PWM) strategies which should be designed to reduce switching losses, leakage current and maximize thermal efficiency. On the other hand, the inverter captures energy released through regenerative breaking and feeds this back to the battery. As a result, the range of the vehicle is directly related to the efficiency of the inverter.

When EV/HEV motor drives operate in high output torque region, the loss and thermal robustness of inverters are an important concerns. Further considering the power density and cost targets of EV/HEV, it is crucial to reduce the inverter switching loss when the output electric current is large (Fig. 1).

Among the disadvantages of Electric Vehicles (EV) is their weak autonomy, whereas for Hybrid Electric Vehicles (HEV) it is the limited space under the hood for another drive train; to improve the autonomy, the battery energy should be used efficiently, on the other hand lower losses would need a smaller and lighter cooling system. In hard switched power converters the switching losses are significantly high, and often represent the bulk of the inverter losses. The greater the switching losses, the greater the need for cooling the power switches. Whereas pulse width modulated converters have carrier and sideband harmonics which is source of electromagnetic pollution which can be divided into two categories, common mode and differential mode noise [1,2].

Space Vector PWM is a digital Power Converter modulation technique where the duty cycle of inverter switches are calculated directly using mathematical transformations based on complex representation of inverter voltages. SVM was chosen over ordinary PWM techniques for the following reasons: better DC voltage utilization [3] and decreased switching losses. Reduced switching losses can be explained by the freedom that one has in generating the pulses when the duty cycles are known before hand [3,4]. The

* Tel.: +33 01 47527291; fax: +33 01 47527012.
E-mail address: el-hadj.miliani@ifpen.fr.

0378-7753/$ – see front matter © 2014 Elsevier B.V. All rights reserved.
http://dx.doi.org/10.1016/j.jpowsour.2014.01.009

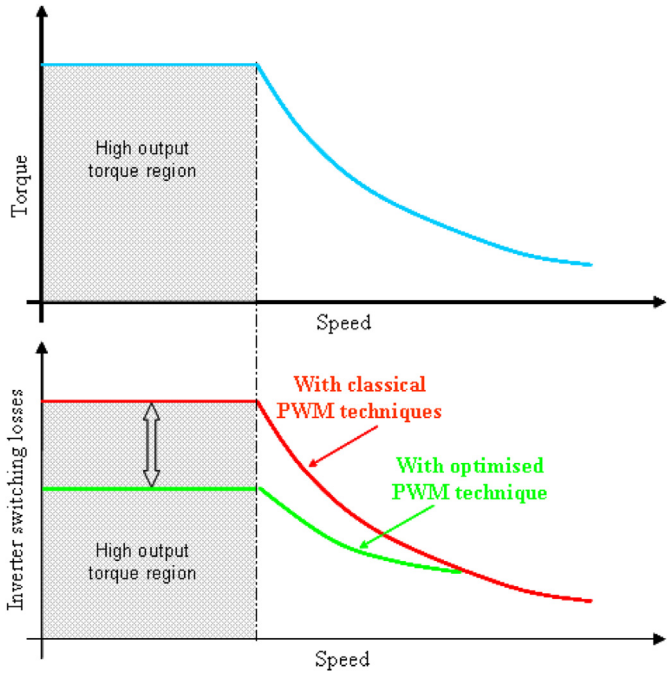

Fig. 1. Switching losses reduction according to torque/speed characteristic for EV/HEV application.

idea is to use the zero vectors (passive vectors) in a way to avoid voltage commutations when it matters the most.

Another weakness of EV and HEV drive train, is the Electro-Magnetic Interference (EMI) aspect which is rarely taken into account at the conception of electric drives which increases the cost and time to market of the drive train due the tedious and tiresome process of EMI suppression [5]. The problem of common mode current or leakage current arises due to the parasitic capacitive coupling between the stator winding and the stator frame (Fig. 2) along with high rate of change of voltage 'dv/dt' in the windings giving path to non negligible common-mode currents (5 A) for switching transients of 200 ns for DC link voltages as low as 200 V. The recent trend of using high speed switches has only worsened

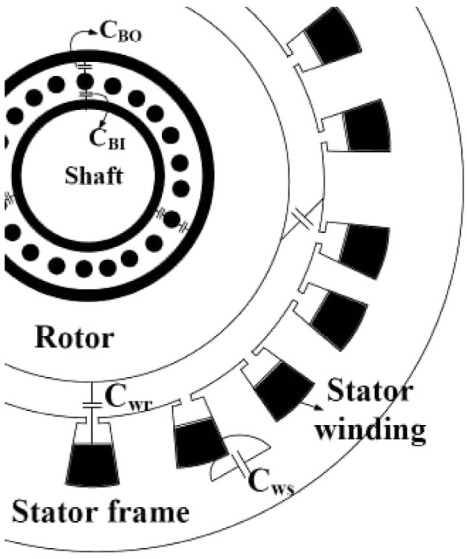

Fig. 2. High frequency representation of an electric drive.

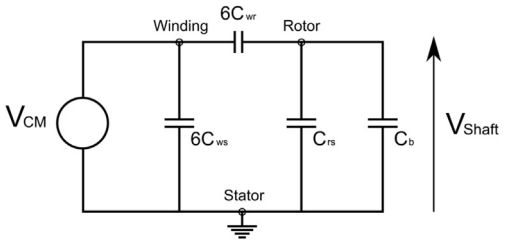

Fig. 3. High frequency equivalent model.

the situation and has created the need for an EM filter to eliminate this noise from the electric drive. In this paper, we present a technique for reducing the leakage current as well as the switching losses.

Some researchers have provided different solutions for these problems; some of them concerning passive and active EMI filters have focused on eliminating high frequency leakage current, shaft voltage and bearing current. Other solutions are based on motor design and variable switching frequency PWM strategies. In Ref. [6], based on the analytical expression of current ripple of common three-phase inverter fed by constant DC-link voltage source, variable switching frequency PWM methods were proposed to effectively reduce the switching losses and/or the conducted EMI noise. Ref. [7] proposes a method for suppressing shaft voltage by modifying the shape of the rotor and the permanent magnets; in order to minimize shaft voltage, a magnet rearrangement and rotor re-structuring of the motor are designed. Ref. [8] proposes a passive cancellation method for the purpose of elimination the adverse effects of PWM inverter in electrical machine system. This method is based on a two small passive EMI filters which can compensate for common mode voltage produced by PWM inverter and leakage current. These methods can effectively reduce the inverter and motor leakage current, the switching losses or system noise. However, these methods are not fit for EV and HEV applications seen on the more weight, volume and cost they introduce. It is more preferable to reduce both the inverter–motor leakage current, switching losses and the system noise by improving the PWM strategy and power components (IGBT) commutations. Taking the EV and HEV application into account, this paper proposes two solutions based on an improved PWM strategy and a technique to control commutation dynamic, which helps to reduce both the inverter switching loss and system leakage current.

This paper includes six parts. First part gives introduction. Second part gives the high frequency behaviour of the drive system. Third part gives the proposed solutions to reduce switching losses and leakage current. Part 4 gives the experimental setup and results for a two level IGBT inverter feeding a 15 kW permanent magnet synchronous motor (PMSM) and finally the conclusion and references are given in part 5 and 6 respectively.

2. High frequency behaviour

Numerous papers have been published by electric drive-train manufacturers in the last several years that attempt to understand the causes of shaft voltage in motors and to find a solution to eliminate electrical bearing damage. Shaft voltage and current flow thru motor bearings represent a significant part of electric drive train problems when operating under Voltage Source Inverter (VSI) controlled with classical PWM techniques.

The shaft voltage magnitude measured is commonly used as an indicator of the possible bearing current that results. It is the magnitude and passage of electrical current thru the bearing that results in a mechanical damage.

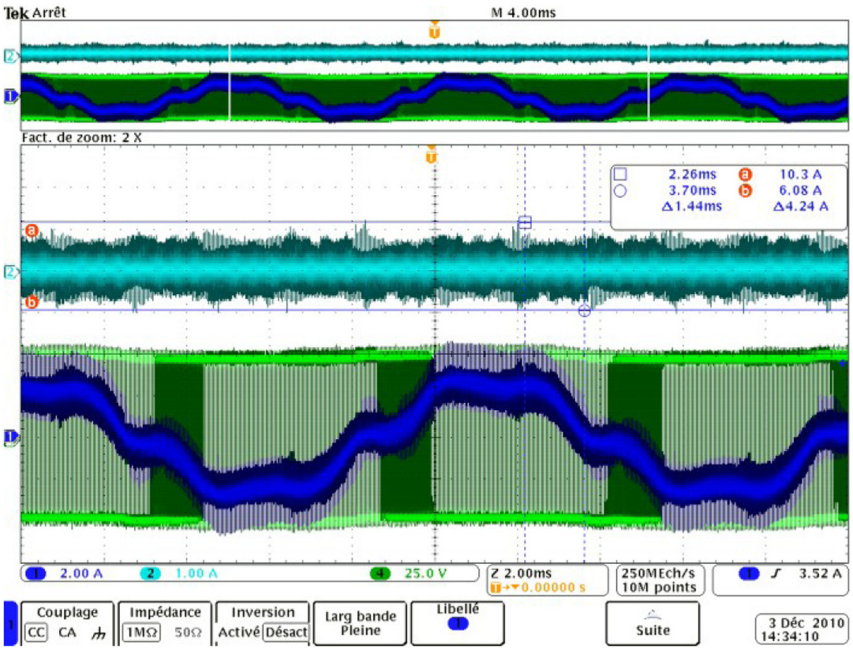

Fig. 4. Leakage current (top), Ia and Va0.

Shaft voltage is proportional to the common mode voltage. Analysing the high frequency circuit a representative electric circuit can be drawn (Fig. 3).

From Fig. 3 we get Equation (1) which shows that linear and proportional relationship of shaft voltage and common mode voltage (V_{CM}).

$$V_{Shaft} = \frac{C_{wr}}{C_{wr} + C_{rs} + C_b} V_{CM} \tag{1}$$

The suffix w, r and s correspond to stator-winding, rotor and stator-frame respectively. This shaft voltage can induce currents between the stator connected to earth and the rotor through the ball bearings. The electric drive topology is a very important factor that needs to be taken into consideration to understand how it affects the generation of V_{CM}.

2.1. Leakage current

A PWM inverter feeding an AC motor often has a problem with a leakage current that flows through the distributed electrostatic capacitance from the motor windings to the ground. A high frequency model of an electrical machine shows a parasitic capacitive coupling between the stator end windings and the stator body [9]. Since the stator is connected to the protective earth and the current leaks into the earth, this is also called common mode current [4,10], this is the main cause of the radiated noise due to the voltage source inverter commutations and coupling elements [11–13]. The expression for the leakage current is given by Equation (2) where C_{ws} is about a few nano-farads for well constructed machine while 'dv/dt' is about 5 GV s^{-1}.

$$I_{leakage} = c_{ws} \frac{dv}{dt} \tag{2}$$

The density of the leakage current depends on the modulation frequency F_{PWM}, pulse positioning technique and the modulation technique used. The modulation frequency determines how frequently the voltage commutations occur, the pulse positioning gives the number of voltage commutations for line voltage, for e.g. pulses placed at the extremes of the modulation period the line voltage have the same number of voltage commutations as the phase voltage while for pulses placed around the centre of the modulation period give twice as many voltage commutations as the phase voltage whereas the type of modulation technique could alter the effective modulation frequency such as in the case of DPWM techniques.

These trends are demonstrated by laboratory tests when using classical modulation technique; natural PWM and without controlling the IGBT commutation speed (by modular gate driver resistance). Results are presented in Fig. 4 in which the curves in green (in the web version) and navy blue are the phase voltage and phase current respectively while the turquoise curve is the leakage current as observed on the test bench.

2.2. Switching losses

In voltage source inverters, the phase voltage generated has only two levels $V_{dc}/2$ and $-V_{dc}/2$ with respect to the DC mid point and since they both have the same absolute value it becomes a constant while calculating the switching losses [14,15]. Hence the only variable is the phase current. Equation (3) gives the switching losses over the fundamental period for a phase.

$$\begin{aligned} P_{sw} &= P_{sw}^{on} + P_{sw}^{off} \\ P_{sw}^{on} &= \frac{f_{sw} V_{dc} t_{rise}}{2} \frac{1}{2\pi} \int_0^{2\pi} |i(t)| dt \\ P_{sw}^{off} &= \frac{f_{sw} V_{dc} t_{fall}}{2} \frac{1}{2\pi} \int_0^{2\pi} |i(t)| dt \end{aligned} \tag{3}$$

IGBT special case: we seldom take into account the effect of out of phase currents (lagging or leading) which necessitate the Free Wheeling Diodes (FWD) to conduct for several commutation periods when the phase voltage and currents are of opposite polarity

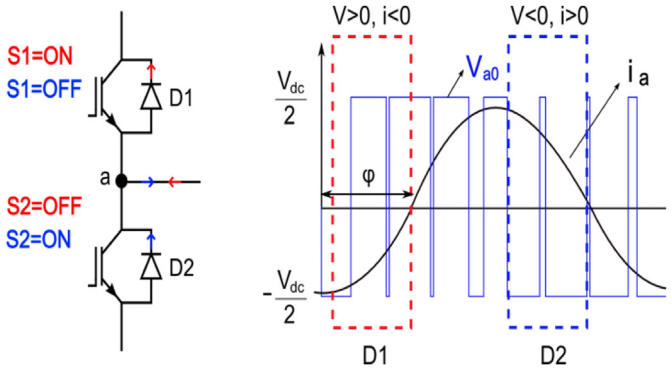

Fig. 5. Free wheeling diodes and out of phase currents.

as IGBTs block reverse current (unlike MOSFET). This means there are less commutation losses during this period because modern FWD such as fast recovery diodes [16], SisC and Schottky diodes, [17] have very low reverse recovery current and lower reverse current peak. The switching losses are much higher in IGBTs than in the FWDs. In this paper, we use this phenomena to our advantage i.e. slow down the switching speed of the IGBT to reduce 'dv/dt' considerably and in turn common mode current and electromagnetic interference (EMI) associated to it, with little effect on the switching losses.

Fig. 5 shows that the diodes not only conduct when the switches are open but also when the current is of the opposite polarity for load angle φ. There are two zones shown on the figure by red (in the web version) and blue rectangles which correspond to the conduction of one of the free wheeling diodes for the negative and positive currents shown by red and blue arrows respectively. Hence there are no switching losses in the IGBTs in these regions but only in the FWD which is comparatively low.

3. Discontinuous space vector PWM and modular gate resistance

Discontinuous modulation techniques or DPWM [18] are the modulation techniques valid for poly-phase loads with a floating neutral i.e. not tied to the ground. The principle of such techniques is to focus on the line voltages rather then phase voltages as it is the potential difference between the phases that matters finally. In this section we have used an evolving (scalable) discontinuous modulation technique with variable switching transients keeping in mind the continuous conduction period of anti-parallel diodes as explained in the previous section.

3.1. Discontinuous space vector PWM

DSVM (Discontinuous SVM) refers to the modulation techniques that use space vector calculation of the active vectors to be applied

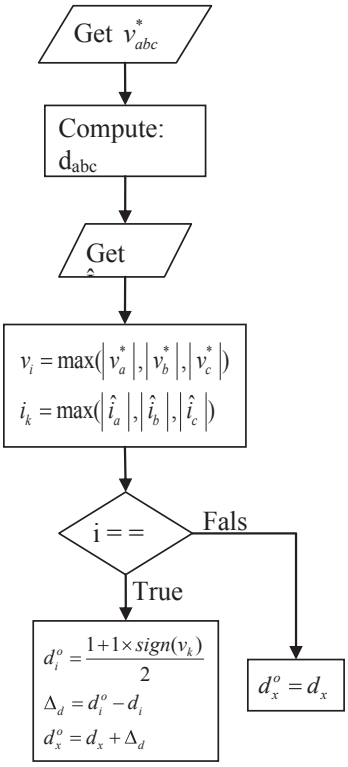

Fig. 7. Algorithm DSVM.

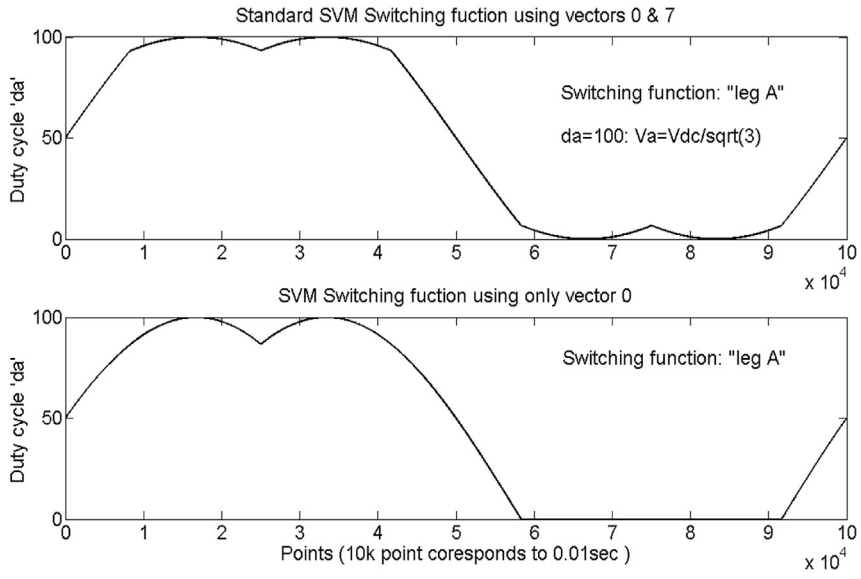

Fig. 6. SVM: switching function leg A.

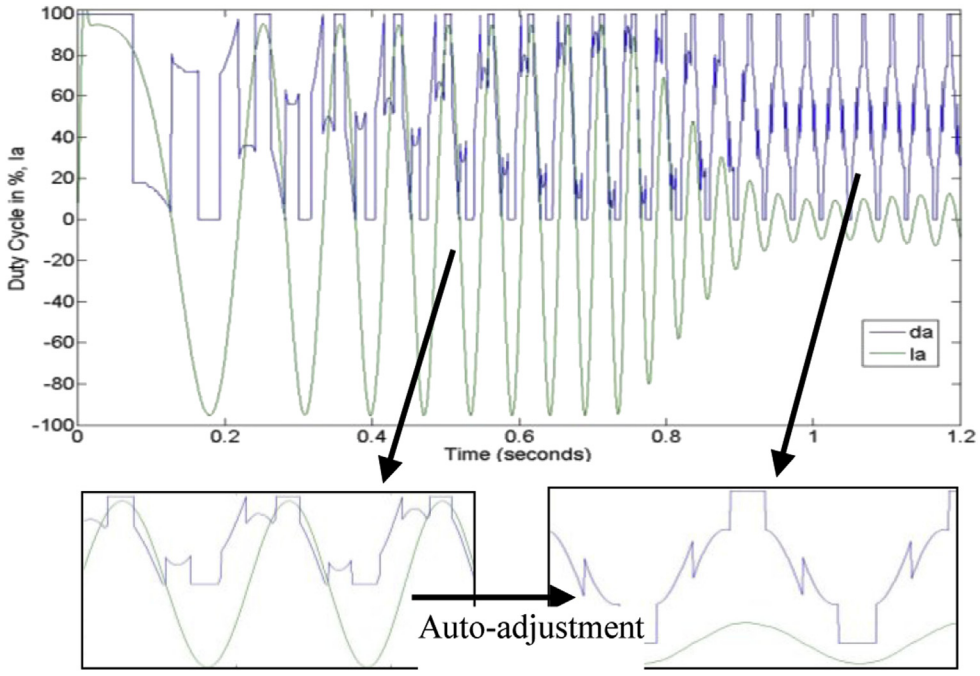

Fig. 8. DSVM: phase current Ia and modulation function for same phase.

and their duty cycles. However the completion of the period using the zero vectors or the sequence of application of the vectors changes to achieve voltage clamping essentially done to decrease the switching losses. The most basic DSVM technique could be achieved using only one of the two zero vectors at a time which would be analogous to DPWMMIN and DPWMMAX if V_0 or V_7 is used respectively.

The zero sequence voltage to be injected to the voltage reference for a Generalized Discontinuous Modulator (GDPWM) for DPWMMIN and DPWMMAX is given by Equations (4) and (5).

$$u_0 = -\frac{V_{dc}}{2} - v_{min} \tag{4}$$

$$u_0 = \frac{V_{dc}}{2} - v_{max} \tag{5}$$

where $v_{min} = \min(v_a^*, v_b^*, v_c^*)$ and $v_{max} = \max(v_a^*, v_b^*, v_c^*)$.

The modulation function for SVM and DSVMMIN is shown in Fig. 6.

A simple yet very effective algorithm shown in Fig. 7 is developed to reduce the switching losses as much as possible using the boundary conditions represented by Equation (6) to clamp a given inverter leg under balanced conditions. The algorithm takes into account the load imbalance as well. If there is a load imbalance, one of the phases will have currents of higher amplitude flowing through it than the other phases and hence higher switching losses and higher thermal stress on the switches of that particular inverter leg which could lead to a failure, Scalable DSVM can avoid such failures by non uniform clamping which would mean an inverter leg will rest idle for a longer duration than the other legs.

$$T_{a\_clamping} = \begin{cases} x, \left(\frac{\pi}{6} \le \omega t < \frac{2\pi}{3} + \frac{\pi}{6}\right) \\ \text{or} \\ x - \frac{2\pi}{3}, \left(\frac{\pi}{6} + \pi \le \omega t < \frac{2\pi}{3} + \frac{\pi}{6} + \pi\right) \end{cases} \tag{6}$$

$x \in \left[0, \frac{2\pi}{3}\right]$

Fig. 8 shows the phase current and modulation function, it can be noticed how the modulation function adapts itself to avoid switching where it would matter the most i.e. at high currents as explained above. A different dead time correction algorithm is used with this technique since there are fewer commutations and different turn *ON* and *OFF* times. The duty cycles are re-adjusted to compensate for the slower commutations. For extreme values (around 0% or 100%) of duty cycle there is a less margin for the compensation hence lesser liberty to slow down the switching without deforming the output voltage.

Fig. 9 shows theoretical results obtained on reduction in the switching losses, the leakage current magnitude and its density for a modulation index of 0.907. The drop in the I_l reduction around 60° (θ, not φ) is due to the presence of the third harmonic component in the phase voltage. Only the first quadrant is shown as the curve is symmetric about $\varphi = 90°$.

3.2. Modular gate resistance

A controllable gate resistor is used which is varied to control the switch ON and OFF time of the IGBTs. Unlike the existing methods,

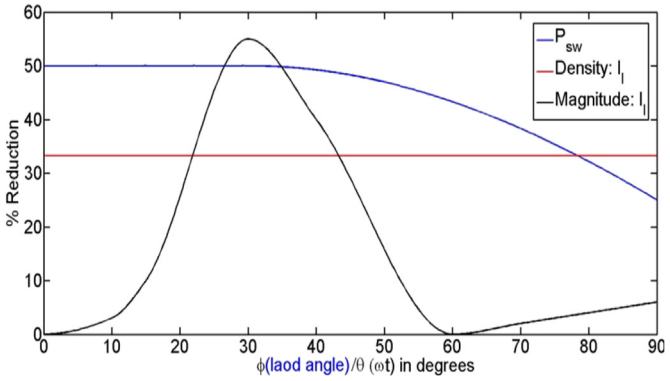

Fig. 9. Switching losses, leakage current magnitude and density reduction.

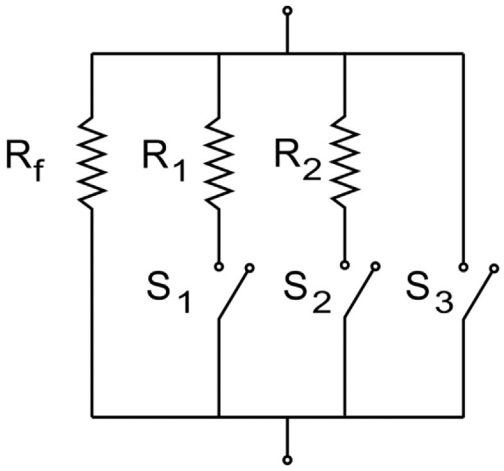

Fig. 10. Circuit for modular gate resistance R_G.

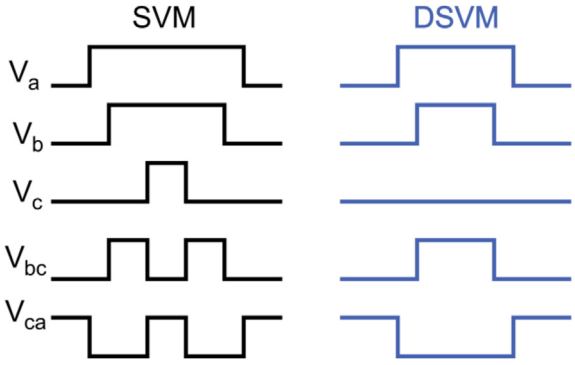

Fig. 11. Line voltage wave form for SVM and DSVM.

in this study a higher value of R_G is used when the anti-parallel diodes conduct or when currents are around zero hence the leakage current is not reduced at the cost of increased switching losses in the IGBTs.

Fig. 10 shows the implementation scheme of the variable gate resistor to be placed at the output of the IGBT driver. This would lead to 8 different configurations and 5 different values ($0, R_f||R_2||R_1, R_f||R_2, R_f||R_1, R_f$) of the equivalent resistance. The slowest and the

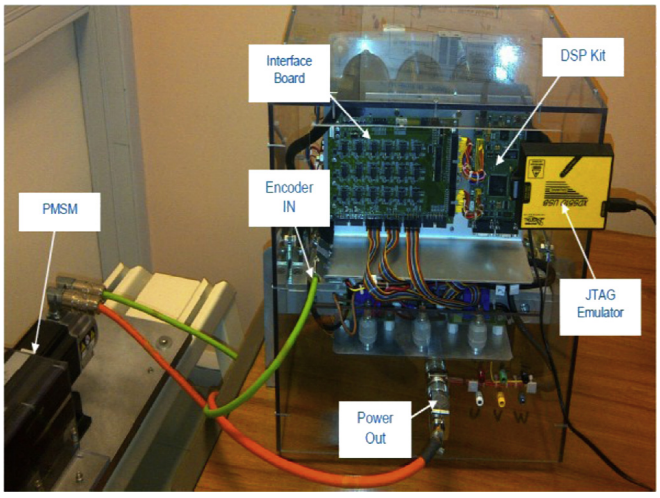

Fig. 13. Test bench.

fastest commutation times all the switches should be open and the switch S3 closed respectively.

3.3. Drawbacks

DSVM has an indirect impact on the quality of the line voltages. The effective line voltage modulation frequency is twice that for standard SVM with centred pulse. It can be seen in Fig. 11 that the line voltages have 2 pulses per PWM period for standard SVM and only one pulse for two of the line voltages for DSVM, where only one zero vector (V_0) is used. It is clear that the volt-seconds for the line voltages are equal in both the cases. This makes the effective modulation frequency smaller by 33.3% for DSVM. This increases the current ripple and in turn the torque ripple.

The ability to slow down the switching speed using this algorithm without significantly increasing the switching losses depends on the load angle so the higher the load angle the higher the liberty to reduce the leakage current. Hence this technique is dependent on the load angle.

3.4. Dead time

For DSVM, an inverter leg stays in the same state for several modulation periods and therefore no dead time effect would be

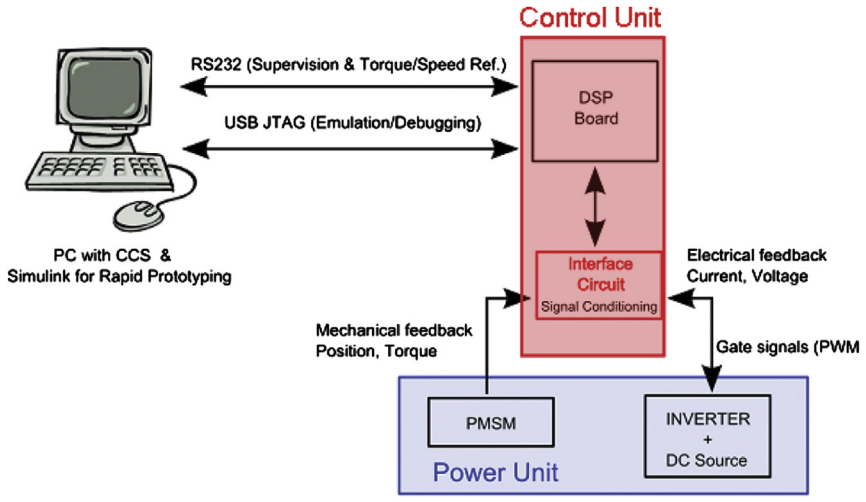

Fig. 12. Power and control units.

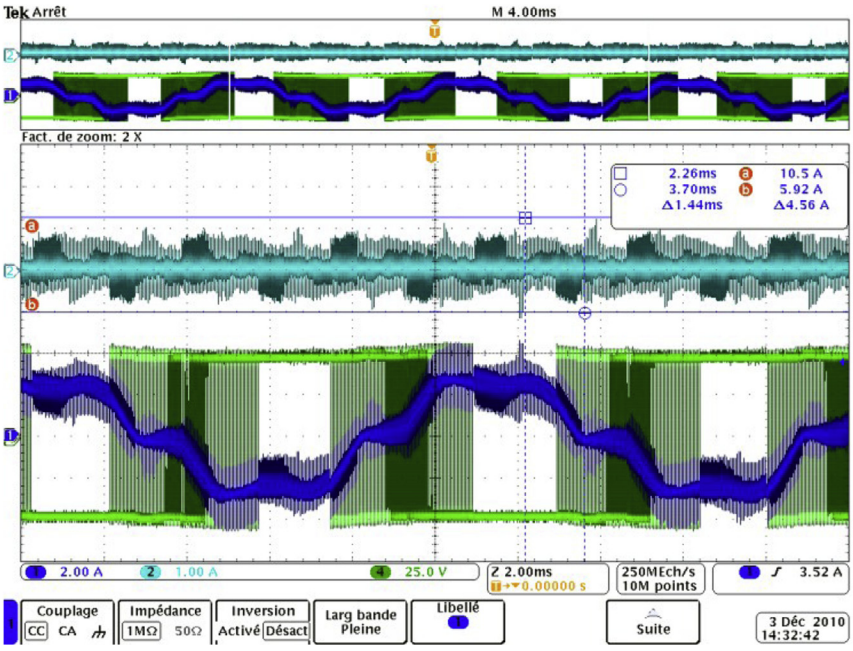

Fig. 14. DSVM Leakage current (top), Ia and Va0.

observed for that leg and no correction is required. Moreover the inverter nonlinearities for extreme values of duty cycles are also reduced, for e.g for a modulation frequency of 20 kHz and a dead time of 1 μs duty cycles smaller than 2% and greater than 98% are as good as 0% and 100% respectively. Thus, for the clamped phase no compensation is required, so standard compensation techniques that adjust the voltage of the phase according to the sign of the phase currents through out the period cannot be used. The low frequency distortion of the phase voltage is alleviated to some extent for discontinuous modulation techniques.

4. Experimental setup and results

The test bench consists of two electric motors mechanically coupled fed by two different inverters controlled independently. One electric drive emulates a variable load to perform different driving cycles and the other drive is the system under observation which consists of a 15 kW, 3-phase 2-level IGBT voltage source inverter (VSI) works on 400 V DC with current, voltage and temperature sensors. The permanent magnet synchronous motor (PMSM) is equipped with an incremental encoder (4096 points) for rotor position measurement. The VSI–PMSM under observation system is controlled by a 150 MHz Floating-Point DSP "TMS320F28335" from Texas Instruments. Necessary signal conditioning components are used to ensure high processing speed and precision in the overall control system. Fig. 12 shows the power and control units of the experimental system.

In order to meet the requirements of our application, the DSP needs to be well initialized (initialization and configuration, synchronization between PWM and ADC module). Based on the specifications of the Field Oriented Control (FOC) and the developed DSVM algorithms, the peripheral unit's configuration are set to the suitable operating modes [19,20].

The objective here is to implement DSVM algorithm which is depicted by the flowchart of Fig. 7. This flowchart details the PWM update after obtaining the phase voltages references from the Field Oriented Control (get V^*_{abc}). After the calculation of duty cycles (d_{abc}) and a phase clamping according to the measured phases currents, an update of the duty cycles is done to scale the phase clamping when necessary. Fig. 13 shows the laboratory experimental test bench.

Fig. 14 in which the green (in the web version) curve is the voltage, navy blue curve the current and the turquoise curve is the leakage current, demonstrates that for high currents the voltage is clamped to either the positive or the negative terminal and therefore discontinuities are clearly visible in the output voltage curve. The leakage current density is now very sparse compared to the results obtained using a standard technique shown in Fig. 4 where the leakage current envelope is consistent and denser.

Global inverter losses are calculated measuring the power supplied by the DC link and comparing it with the power at the inverter legs for the proposed and the standard technique. The losses in the IGBT drivers are not taken into account. Table 1 shows results using scalable DSVM, as expected at higher switching frequencies we observe an increase in the contrast between the two techniques in terms of losses. The global inverter losses are further reduced which means that while the conduction losses remain constant the switching losses increase with increase in frequency. However, it should be noted that the absolute inverter losses increase with an increase in the switching frequency.

Table 1
Losses reduction, experimental results.

Frequency kHz	% Loss reduction
15	12.98
25	20.75
35	22.85

5. Summary

In this paper, discontinuous space vector PWM strategy and a variable gate resistor technique are proposed for EV/HEV drivetrain; the proposed methods can effectively reduce the inverter switching loss and leakage current. Experimental results show a decrease in global inverter losses from 7.18% to 5.69% which translates to an overall reduction of inverter losses by 20.75% for a

switching frequency of 25 kHz. Leakage current density was reduced by 33% with smaller peaks around phase current zero crossing. Since the electric motor is a dynamic inductive load, the load angle 'φ' varies with the output frequency or the machine speed and determines the extent to which the switching transients could be slowed to reduce the leakage current without increasing the switching losses. However discontinuous modulation techniques have some drawbacks too, so in the end a compromise has to be made between torque ripple and switching losses.

References

[1] Maria Carmela Di Piazza, Antonella Ragusa, Gianpaolo Vitale, IEEE Trans. Veh. Technol.. ISSN: 00189545 59 (6) (2010) 2664.
[2] D. Grahame Holmes, Thomas A. Lipo, IEEE Press Power Eng. (2003).
[3] H.W. van der Broeck, H.C. Skudelny, G.V. Stanke, IEEE Trans. Ind. Appl. 24 (1) (Jan–Feb. 1988).
[4] A. Kolli, O. Bethoux, A. De Bernardinis, E. Labouré, G. Coquery, IEEE Trans. Veh. Technol. (2013), 99.
[5] Firuz Zare, IEEE EMC Soc. Newslett. (2009) 66–70.
[6] X. Mao, R. Ayyanar, H.K. Krishnamurthy, IEEE Trans. Power Electron. 24 (4) (Apr. 2009) 991–1001.
[7] K. Kyung-Tae, C. Sang-Hoon, H. Jin, S. Jae-Sun, K. Byeong-Woo, J. Electr. Eng. Technol. 8 (4) (2013).
[8] X. Chen, D. Xu, F. Liu, J. Zhang, IEEE Trans. Ind. Electron. 54 (1) (2007) 419–426.
[9] H. Akagi, S. Tamura, IEEE Trans. Power Electron. (2006).
[10] N. Idir, Y. Weens, M. Moreau, J.J. Franchaud, IEEE Trans. Magn. 45 (1) (Jan. 2009) 133–138. Part 1.
[11] Firuz Zare, IEEE EMC Soc. Newslett. (Summer 2009) 53–58.
[12] Sabine Marksell, EMC Aspects of PWM Controlled Loads in Vehicles, PhD thesis, Department of Industrial Electrical Engineering and Automation, LUND University, 2004.
[13] N. Mutoh, IEEE Trans. Veh. Technol. 57 (4) (2007) 2089–2098.
[14] J.O. Estima, A.J. Marques Cardoso, IEEE Trans. Veh. Technol. 61 (3) (2012) 1021–1031.
[15] J.W. Kolar, H. Ertl, F.C. Zach, IEEE Trans. Ind. Appl. 27 (1991) 1063–1075.
[16] G. Li, Z.Q. Liu, A. Golland, F. Wakeman, in: European Conference on Power Electronics and Applications, Dresden, 2005.
[17] John W. Palmour, in: Compound Semiconductor Integrated Circuit Symposium (CSIC), San Antonio, 2006.
[18] Ahmet M. Hava, Russel J. Kerkman, Thomas A. Lipo, IEEE Trans. Ind. Appl. 34 (5) (September/October 1998).
[19] I. Colak, E. Kabalci, J. Power Sources 196 (18) (15 September 2011) 7585–7593.
[20] W. Shireen, S. Vanapalli, H. Nene, J. Power Sources 166 (2) (15 April 2007) 445–449.